RSC Advances

PAPER

View Article Online
View Journal | View Issue

Cite this: *RSC Adv.*, 2017, **7**, 38044

Wide band gap design of new chalcogenide compounds: $KSrPS_4$ and $CsBaAsS_4$†

Jianqiao Jiang,[a] Dajiang Mei,*[a] Pifu Gong,[bd] Zheshuai Lin,[b] Junbo Zhong[c] and Yuandong Wu[a]

Received 25th January 2017
Accepted 19th July 2017

DOI: 10.1039/c7ra01142c

rsc.li/rsc-advances

Recently, the exploration of infrared nonlinear optical (IR NLO) materials has mainly focused on chalcogenide compounds. However, their practical applications are often hampered by the low laser damage thresholds (LDTs). It is known that wide band gaps can significantly enhance the LDTs of materials, and the introduction of alkali and alkaline earth cations would broaden the band gap. Accordingly, in this work two new compounds $KSrPS_4$ and $CsBaAsS_4$ with both alkali and alkaline earth cations were synthesized successfully. Both compounds crystallize in the space group *Pnma* (62) of the orthorhombic system, and the structures consist of isolated PnS_4 (Pn = P, As) tetrahedra with the interstices occupied by K (or Cs) and Sr (or Ba) atoms, respectively. The band gaps of compounds were determined by different methods. The UV-visible diffuse reflectance spectra revealed that the band gaps of $KSrPS_4$ and $CsBaAsS_4$ are larger than 3.62 eV and 2.86 eV, respectively. The band gaps are primarily determined by the PnS_4 tetrahedra.

Introduction

It is well known that coherent IR lasers have been widely applied in civil and military fields such as laser guidance, signal communication and industrial processing. A number of NLO materials have been applied to generate IR lasers. The commercial IR NLO materials are mainly focused on chalcogenide compounds, such as $AgGaS_2$ and $AgGaSe_2$,[1,2] which have been applied in optoelectronic and thermoelectric areas because of their diverse structures and physical properties.[3–8] However, these materials suffer from the low LDTs, which limits their further application in various areas. Here, the low LDT is principally caused by the relatively small band gap of the material. Materials with higher LDTs can be obtained based on broader band gaps. Numerous research has been conducted to search for novel, promising mid-IR NLO materials that exhibit broad band gaps and strong NLO responses.[9–29] In our previous research for $Ag_3Ga_3SiSe_8$ and $AgGaSiSe_4$ compounds, it mentioned that the band gap of material can be enlarged through the introduction of the Ge or Si element.[24,25] And compared to the band gap of $AgGaSe_2$ (ref. 2) with 1.8 eV, the band gaps of $AgGaSiSe_4$ (ref. 24) and $Ag_3Ga_3SiSe_8$ (ref. 25) are broadened to 2.63 eV and 2.30 eV, respectively. The introduction of alkali or alkaline earth cations which usually are electropositive elements also contributes to broaden band gap of materia.[26–28] For example, the band gaps of $BaGa_4S_7$ (ref. 26) and $LiGaS_2$ (ref. 27) increased to 3.54 eV and 4.15 eV, respectively, compared to that of $AgGaS_2$ with 2.75 eV. Those of $BaGa_4Se_7$ (ref. 28) and $LiGaSe_2$ (ref. 27) increased to 2.64 eV and 3.34 eV, respectively, compared to that of $AgGaSe_2$ with 1.8 eV. And with the introduction of both alkali and alkaline earth cations, the band gap of Na_2BaGeS_4 (ref. 29) reached 3.7 eV. Wherefore in this work, we attempted to simultaneously introduce the alkali and alkaline earth cations to broaden the band gap of material. Meanwhile the introduction of PnS_4 (Pn = P, As) groups are conducive to improve the NLO properties.[30] Through the combination of alkali and alkaline earth cations with the PnS_4 groups, we conducted the research to the A/AL/Pn/S (A = alkali cations, AL = alkaline earth cations) system, and fortunately, the two new compounds $KSrPS_4$ and $CsBaAsS_4$ were successfully synthesized. The syntheses, crystal structures, electronic structures and optical properties of the materials were also investigated.

Experimental section

Synthesis

The compound $KSrPS_4$ was prepared by combining K_2S_3 (prepared by stoichiometric reaction of the K (Sinopharm

[a]College of Chemistry and Chemical Engineering, Shanghai University of Engineering Science, Shanghai 201620, P. R. China. E-mail: meidajiang718@pku.edu.cn
[b]Center for Crystal Research and Development, Key Laboratory of Functional Crystals and Laser Technology, Chinese Academy of Sciences, Beijing 100190, P. R. China
[c]Key Laboratory of Green Catalysis of Higher Education Institutes of Sichuan, College of Chemistry and Environmental Engineering, Sichuan University of Science and Engineering, Zigong 643000, P. R. China
[d]University of Chinese Academy of Sciences, Beijing 100190, P. R. China

† Electronic supplementary information (ESI) available: Crystallographic data in CIF format for $KSrPS_4$ and $CsBaAsS_4$. CCDC 1502143 and 1503947. For ESI and crystallographic data in CIF or other electronic format see DOI: 10.1039/c7ra01142c

chemical Reagent Co., Ltd., 98%) and S (Sinopharm chemical Reagent Co., Ltd., 99.5%) elements in liquid NH_3), SrS (prepared by stoichiometric reaction of Sr (Sinopharm chemical Reagent Co., Ltd., 99%) and S elements), Nd (Sinopharm chemical Reagent Co., Ltd., 99.9%), P_2S_5 (Sinopharm chemical Reagent Co., Ltd., 99%) and additional S (Sinopharm chemical Reagent Co., Ltd., 99.5%) in the molar ratio 2 : 1 : 1 : 1 : 6. The sample was heated in a computer-controlled furnace to 973 K, then kept there for 5 d, then cooled to 373 K at the rate of 3 K h^{-1}. The resulting melts were washed with dimethylformamide (DMF) and acetone in turn. The product consisted of colorless transparent platelet $KSrPS_4$. This compound was stable in dry air for several days.

The compound $CsBaAsS_4$ was prepared by combining Cs_2S_3 (prepared by stoichiometric reaction of the Cs (Alfa Aesar, 99.8%) and S (Sinopharm chemical Reagent Co., Ltd., 99.5%) elements in liquid NH_3), BaS (Sinopharm chemical Reagent Co., Ltd., 99%), Nd (Sinopharm chemical Reagent Co., Ltd., 99.9%), As_2S_3 (Sinopharm chemical Reagent Co., Ltd., 99%) and additional S (Sinopharm chemical Reagent Co., Ltd., 99.5%) in the molar ratio 2 : 0.5 : 1 : 1 : 6. The sample was heated in a computer-controlled furnace to 973 K, then kept there for 5 d, then cooled to 373 K at the rate of 3 K h^{-1}. The resulting melts were washed with DMF and acetone in turn. The product consisted of yellow transparent platelet crystal of $CsBaAsS_4$. This compound was stable in dry air for several days.

Energy dispersive X-ray fluorescence test

The analysis of the compounds was carried out with Shimadzu EDX-720 Energy Dispersive X-ray Fluorescence spectrometer. The tests for each compound were performed with 5 times, and the spectra of number 1 and 6, as shown in Fig. 1 (the rest of the number 2–5 and 7–10 spectra are shown in the ESI†), manifested the presence of K, Sr, P, S and Ca, Ba, As, S in the approximate molar ratio of 1 : 1 : 1 : 4 and 1 : 1 : 1 : 4, respectively.

Single crystal data collection

Single crystal X-ray diffraction data were collected with graphite-monochromatized Mo K radiation ($\lambda = 0.71073$ Å) at 220 K on a STOE Imaging Plate Diffraction System (IPDS-1).

UV-vis diffuse reflectance test

UV-vis diffuse reflectance spectroscopy test was performed on a Shimadzu UV-3600 spectrophotometer. The samples and $BaSO_4$ (totally reflected) were ground together at room temperature. Then the mixture was prepared as a flat specimen, and in UV/vis range, the resolution was 0.1 nm. The data were collected at 200–800 nm.

Second harmonic generation test

The optical second harmonic generation test was performed on the powder sample of $KSrPS_4$ and $CsBaAsS_4$ by means of the Kurtz–Perry method,[31] with a 1.06 μm Q-switch laser. The samples were ground and sieved by using a series of mesh sizes in the range of 80–100 μm. Similar size of $AgGaS_2$ was chosen as the reference.

Laser damage threshold test

The laser damage thresholds of title compounds were evaluated on powder sample with a pulsed YAG laser (1.06 μm, 10 ns, 10 Hz).[32] Similar size of $AgGaS_2$ was chosen as the reference.

Structure determination

The structure model was obtained by direct methods and was refined by full-matrix least-squares refinement based on F2 using the Shelxtl package.[33] The positions were standardized with the Structure Tidy program within the Platon package.[34] The final refinement converged with a residual factor of $wR_2 = 0.095$ (all data). Technical details of the data acquisition as well as some refinement results are summarized in Table 1.

The first-principles calculations

The first-principles calculations for the $KSrPS_4$ and $CsBaAsS_4$ crystals are performed by the plane-wave pseudo potential method implemented in the CASTEP package based on the density functional theory (DFT).[35] The ion–electron interactions are modeled by the optimized normal-conserving pseudo potentials for all elements. The adopted density functional method is exchange-correlation (XC) functional of local density approximation (LDA).[36] The kinetic energy cutoffs of 800 eV and Monkhorst–Pack *k*-point meshes[37] with density of (2 × 3 × 2) and (1 × 3 × 3) points in the Brillouin zone are chosen for $KSrPS_4$ and $CsBaAsS_4$ crystals, respectively. Our tests reveal that the above computational set ups are sufficiently accurate for the present purposes.

Results and discussion

The two compounds $KSrPS_4$ and $CsBaAsS_4$ crystallize in space group *Pnma* (62) of the orthorhombic system and adopt the $TlEuPS_4$ (ref. 38) structure type, As shown in Fig. 2. The structures consist of isolated PnS_4 (Pn = P, As) tetrahedra separated by the K (or Cs) and Sr (or Ba) atoms, and the atoms locate in the tunnel formed by the tetrahedra, respectively. The asymmetric units for both compounds contain one crystallographically independent K (or Cs) atom, one independent Sr (or Ba) atom, one independent P (or As) atom and three independent S atoms.

For $KSrPS_4$, K atom is coordinated to a bicapped trigonal prism of eight S atoms with K–S distances ranging from 3.336(1) to 3.603(2) Å, which is close to those of 3.2058(14)–3.5239(14) Å for K–S distances in $KBiSiS_4$ (ref. 39) and 3.194(3)–3.601(3) Å for K–S distances in $KBiGeS_4$.[39] The Sr atom is coordinated to 9 S atoms with Sr–S distances ranging from 2.992(1) to 3.685(1) Å, which is close to those of 2.928–3.242 Å for Sr–S distances in Sr_2ZnS_3.[40] Each P atom is bonded to four S atoms to form a slightly distorted tetrahedron, with the bond lengths ranging from 2.023(2) to 2.049(8) Å, similar to those of 2.010(1)–2.090(1) Å for P–S distances in $LiZnPS_4$.[41] Since S–S bonds are not observed in the structure, the oxidation states of 1+, 2+, 5+, 2− can be distributed to K, Sr, P and S, respectively.

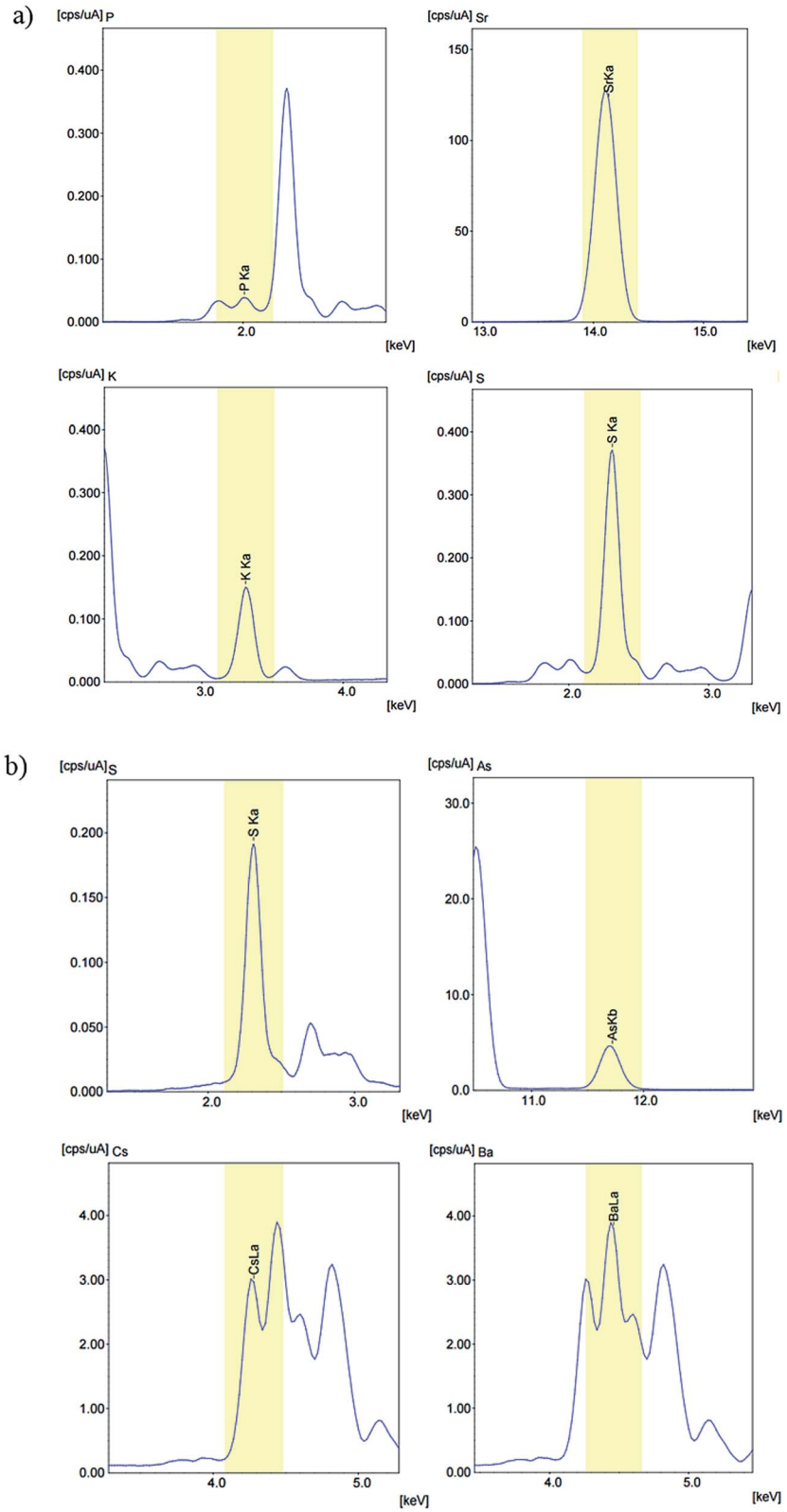

Fig. 1 (a) Energy dispersive X-ray fluorescence spectra of $KSrPS_4$, (b) energy dispersive X-ray fluorescence spectra of $CsBaAsS_4$.

For $CsBaAsS_4$, Cs atom is bonded to 10 S atoms with Cs–S distances ranging from 3.468(2) to 3.895(1) Å, which is close to those of 3.4022(10)–4.0982(13) Å for Cs–S distances in $Cs_3Bi(AsS_4)_2$.[42] While Ba is coordinated to 9 S atoms with Ba–S distances ranging from 3.182(2) to 3.588(0) Å, similar to those of 2.896(2)–3.331(2) Å for Ba–S distances in $Ba_{23}Ga_8Sb_2S_{38}$.[43] Each

Table 1 Crystal data and structure refinement for $KSrPS_4$ and $CsBaAsS_4$

	$KSrPS_4$	$CsBaAsS_4$
F_w (g mol^{-1})	285.93	473.41
a (Å)	16.8214(9)	11.9066(6)
b (Å)	6.6274(5)	6.9184(5)
c (Å)	6.5585(4)	10.0338(5)
V (Å^3)	731.16(8)	826.53(8)
Space group	*Pnma* (62)	*Pnma* (62)
Z	4	4
Index ranges	$-21 \le h \le 22$	$-15 \le h \le 15$
	$-8 \le k \le 8$	$-9 \le k \le 9$
	$-8 \le l \le 8$	$-13 \le l \le 12$
Theta range	2.42–28.08	2.65–28.08
Number of reflection collected	873	1029
ρ_c (g cm^{-3})	2.598	3.804
μ (cm^{-1})	91.84	140.24
$R(F)^a$	0.0292	0.0309
$R_w(F_o^2)^b$	0.0770	0.0775

^{a} $R(F) = \sum||F_o| - |F_c||/\sum|F_o|$ for $F_o^2 > 2\sigma(F_o^2)$. ^{b} $R_w(F_o^2) = \{\sum[w(F_o^2 - F_c^2)^2]/\sum wF_o^4\}^{1/2}$ for all data.

As atom is bonded to four S atoms to form a slightly distorted tetrahedron, with the As–S bond lengths ranging from 2.153(4) to 2.161(1) Å, which is similar to those of 1.918(3)–2.390(3) Å for As–S distances in $Cs_3Bi(AsS_4)_2$ and 2.229(2)–2.266(2) Å for As–S distances in $Cs_3Ta_2AsS_{11}$.[44] Since S–S bonds are not observed in the structure, the oxidation states of 1+, 2+, 5+, 2− can be distributed to Cs, Ba, As and S, respectively.

For these compounds, the larger content of alkali cations (K, Cs) and alkaline cations (Ba, Sr) is, the sparser the PS_4 and AsS_4 tetrahedra connectivity will be, which can be referred to our previous work on $Ba_5Al_2Se_8$ and $Ba_5Ga_2Se_8$.[45] And the tetrahedra would be completely separated from each other by the K (or Cs) and Sr (or Ba) atoms.

From the UV-visible diffuse reflectance spectra of the compounds in Fig. 3(a), the absorption edges are about 343 nm and 434 nm for $KSrPS_4$ and $CsBaAsS_4$, respectively. The band gaps of $KSrPS_4$ and $CsBaAsS_4$ obtained by direct extrapolation method[46] with baseline tangents were 3.62 and 2.86 eV, respectively. To correctly compared the band gaps of different compounds, the measurement methods need to be consistent. And in the Fig. 3(b), the direct extrapolation method with upper tangents were carried out on the spectra, and the results showed that the band gaps of compounds are 4.23 eV and 3.25 eV, respectively. These two compounds band gaps are significantly larger than that of the commercial materials $AgGaS_2$ (ref. 1) with 2.75 eV and $AgGaSe_2$ (ref. 2) with 1.8 eV. The band gaps of $KSrPS_4$ and $CsBaAsS_4$ are also larger than that of $BaGa_4S_7$ (ref. 26) with 3.54 eV and $BaGa_4Se_7$ (ref. 28) with 2.64 eV, respectively, indicated that compounds with large band gaps were obtained. According to the single crystal growth experiment results, the colors for $KSrPS_4$ and $CsBaAsS_4$ crystals are colorless and yellow

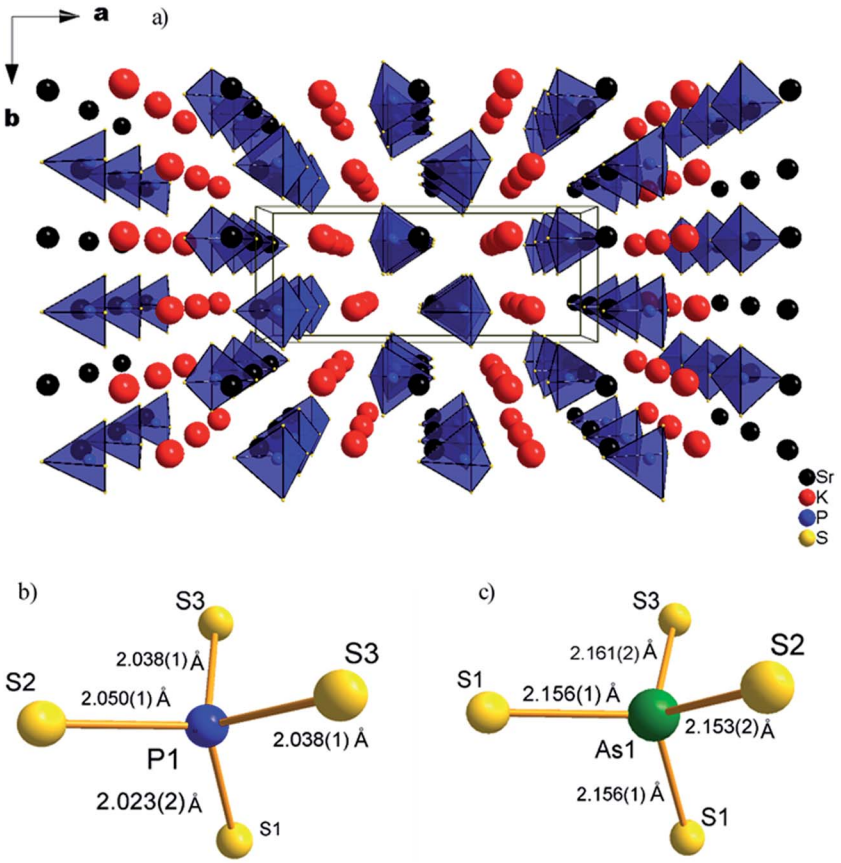

Fig. 2 (a) Unit cell structure of $KSrPS_4$, (b) PS_4 tetrahedron in $KSrPS_4$ structure, and (c) AsS_4 tetrahedron in $CsBaAsS_4$ structure.

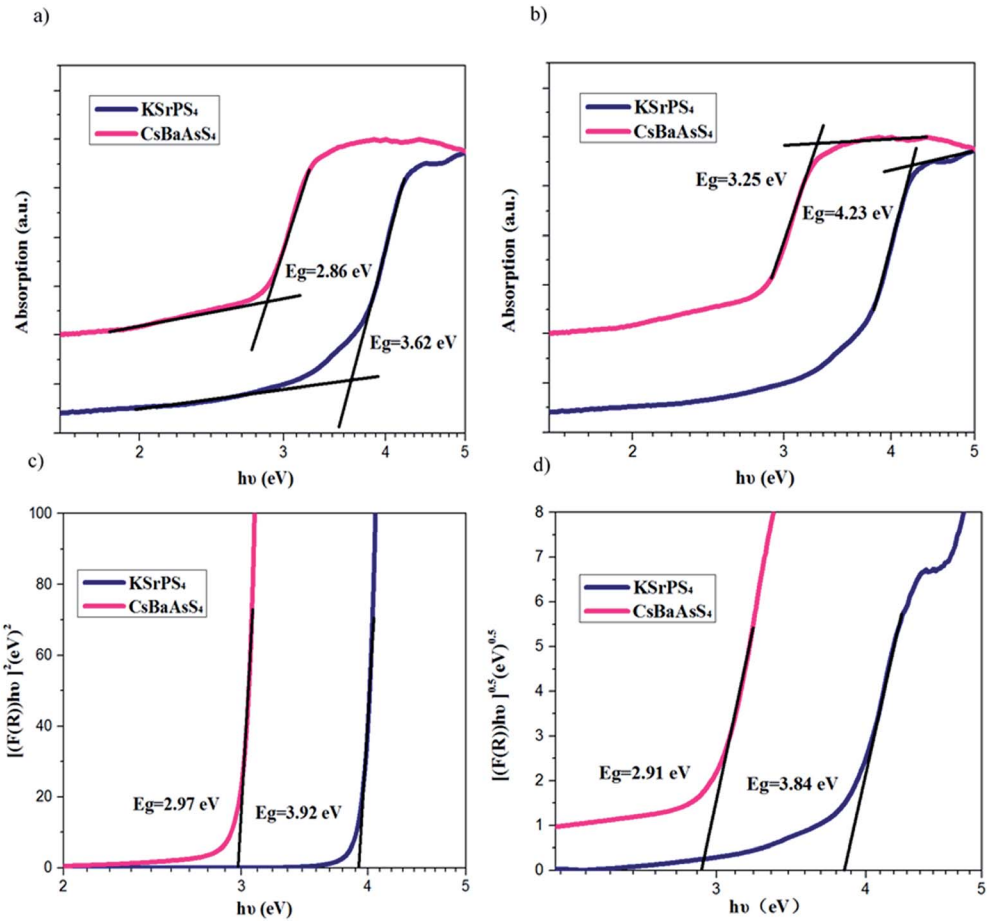

Fig. 3 Diffuse spectra of $KSrPS_4$ and $CsBaAsS_4$: (a) the spectra with upper tangents; (b) the spectra with baseline tangents; (c) the spectra of $(F(R)\ h\upsilon)^2$ *versus* hυ; (d) the spectra of $(F(R)\ h\upsilon)^{0.5}$ *versus* $h\upsilon$.

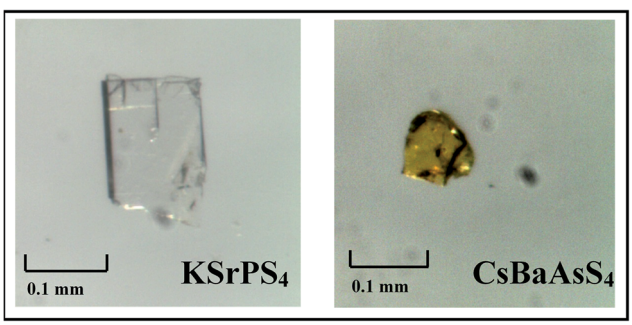

Fig. 4 The single crystals of $KSrPS_4$ and $CsBaAsS_4$ compounds.

(see in Fig. 4), respectively, which was in good accordance with the UV-visible reflectance spectra. In the Fig. 3(c) and (d), the direct and indirect band gaps are measured by Tauc–Davis Mott expressions.[47] The measurement of direct band gap indicated that $KSrPS_4$ and $CsBaAsS_4$ is 3.92 eV and 2.97 eV, respectively. And the measurement of indirect band gap indicated that $KSrPS_4$ and $CsBaAsS_4$ is 3.84 eV and 2.91 eV, respectively.

The laser damage test was performed on the powder sample with a pulsed YAG laser (1.06 μm, 10 ns, 10 Hz). $AgGaS_2$ was served as the reference. The results showed that both the laser damage thresholds of $KPSrS_4$ and $CsBaAsS_4$ are above 5 times of that of $AgGaS_2$. The optical second harmonic generation test was performed on $KSrPS_4$ and $CsBaAsS_4$ with a 1.06 μm Q-switch laser. The compounds $KSrPS_4$ and $CsBaAsS_4$ did not give any second harmonic generation signal because of their centrosymmetric structure.

The electronic band structures of the $KSrPS_4$ and $CsBaAsS_4$ crystals are shown in Fig. 5. The calculations with sX-LDA functional were carried out to investigate the experimental values of band gaps and the results showed the values of 3.58 eV and 2.73 eV for $KSrPS_4$ and $CsBaAsS_4$, respectively.

The partial density of state (PDOS) projected on the constitutional atoms of the $KSrPS_4$ and $CsBaAsS_4$ are shown in Fig. 6, from which several electronic characteristics are shown: (i) the region lowered than −5 eV consist of the isolated inner-shell states with K 2s2p (or Cs 5s5p), Sr 4s4p (or Ba 5s5p), P 3s2p (or As 4s3p) and S 3s2p orbitals, which have little interaction with neighbor atoms. (ii) The upper part of the valence band (about −4 eV) is mainly composed of the p orbitals of P 3p (As 4p) and S 3p orbitals, but the extra top of the VB is occupied by the S 3p orbitals. (iii) Although all the elements contribute to the states on the bottom of conduct band, states on the bottom of conduct band mostly come from the S and P (As) atoms.

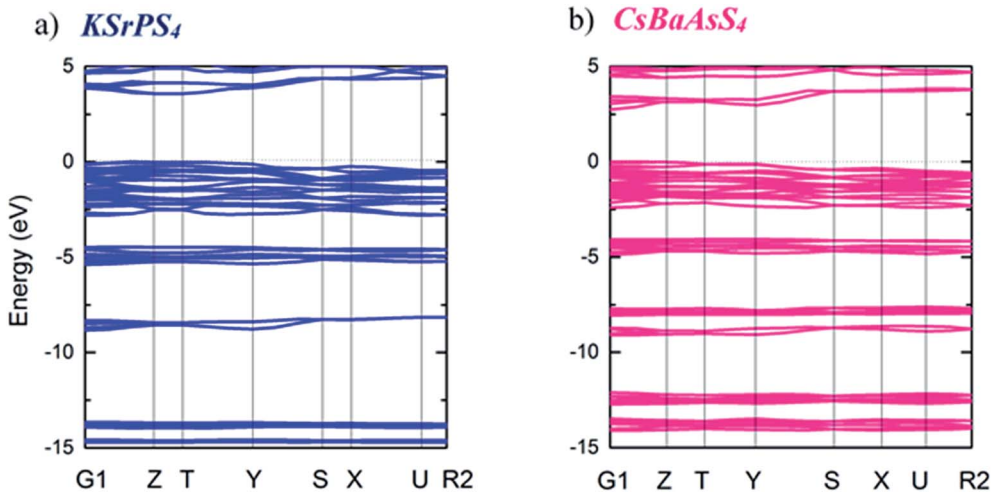

Fig. 5 (a) The band structure of $KSrPS_4$, and (b) band structure of $CsBaAsS_4$.

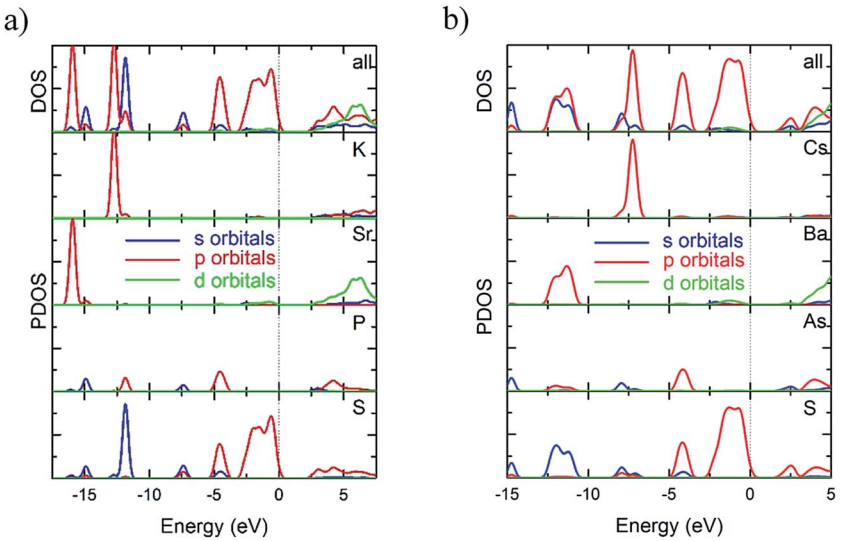

Fig. 6 (a) The PDOS of $KSrPS_4$, and (b) PDOS of $CsBaAsS_4$ crystals.

In summary, the upper part of valence band and the bottom of conduct band are principally determined by the P (As) and S elements, which indicated that the optical absorption is mostly determined by $(PnS_4)^{3-}$ (Pn = P, As) groups.

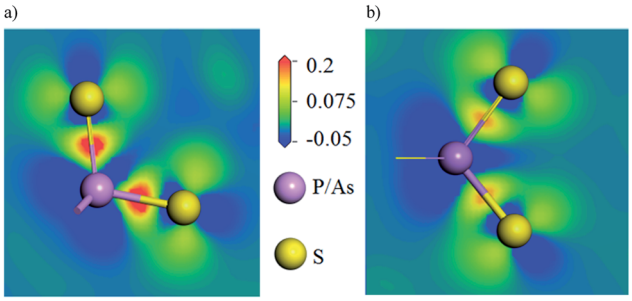

Fig. 7 (a) The electronic charge density difference plotting on the PS_4 groups, and (b) AsS_4 groups.

To further investigate the relationship between the structures and properties of the compounds, the contours of electronic density difference on the PS_4 and AsS_4 groups were drawn for the title compounds in Fig. 7, which illustrate charge redistribution due to the formation of chemical bonds. It is obvious that more charges are located on the P–S bonds than on the As–S bonds, indicating the much stronger covalent characteristic of the former chemical bonds.

Conclusions

To obtain compounds with wide band gaps, in this work, introduction of both the alkali and alkaline earth cations was carried out. Two new compounds $KSrPS_4$ and $CsBaAsS_4$ were successfully synthesized. The compounds crystallize in space group *Pnma* (62) of the orthorhombic system and adopt the $TlEuPS_4$ structure type. The band gaps of compounds were

determined by four methods. The results revealed that the band gaps of $KSrPS_4$ and $CsBaAsS_4$ are larger than 3.62 eV and 2.86 eV, respectively, which imply that the band gaps of compounds were successfully broadened compared with the commercial materials $AgGaS_2$ and $AgGaSe_2$, respectively. The band gaps are primarily determined by the PnS_4 (Pn = P, As) tetrahedra. Such compounds may arouse further interest in exploring new IR NLO materials with wide band gaps, through introducing the alkali or alkaline earth cations.

Acknowledgements

This research was supported by the National Natural Science Foundation of China (No. 51502169), China "863" project (No. 2015AA034203), Opening Project of Key Laboratory of Green Catalysis of Sichuan Institutes of High Education (No. LZJ1503), Shanghai University of Engineering Science "Innovation Training Project of Undergraduate" (No. cs1504002) and Shanghai University of Engineering Science "Scientific Research Training Project of Undergraduate" (No. HZJY20160029).

References

1 D. Chemla, P. Kupecek, D. Robertson and R. Smith, *Opt. Commun.*, 1971, **3**, 29.
2 R. K. Route, R. S. Feigelson and R. J. Raymakers, *J. Cryst. Growth*, 1974, **24**, 390.
3 K. Ramanathan, M. A. Contreras, C. L. Perkins, S. Asher, F. S. Hasoon, J. Keane, D. Young, M. Romero, W. Metzger, R. Noufi, J. Ward and A. Duda, *Prog. Photovoltaics*, 2003, **11**, 225.
4 K. Biswas, J. He, I. D. Blum, C.-I. Wu, T. P. Hogan, D. N. Seidman, V. P. Dravid and M. G. Kanatzidis, *Nature*, 2012, **489**, 414.
5 Y. Pei, X. Shi, A. LaLonde, H. Wang, L. Chen and G. J. Snyder, *Nature*, 2011, **473**, 66.
6 S. N. Guin, A. Chatterjee, D. S. Negi, R. Datta and K. Biswas, *Energy Environ. Sci.*, 2013, **6**, 2603.
7 S. Roychowdhury, U. S. Shenoy, U. V. Waghmare and K. Biswas, *Angew. Chem., Int. Ed.*, 2015, **54**, 15241.
8 S. N. Guin, J. Pan, A. Bhowmik, D. Sanyal, U. V. Waghmare and K. Biswas, *J. Am. Chem. Soc.*, 2014, **136**, 12712.
9 W. Yin, K. Feng, R. He, D. Mei, Z. Lin, J. Yao and Y. Wu, *Dalton Trans.*, 2012, **41**, 5653.
10 Z.-Z. Luo, C.-S. Lin, W.-L. Zhang, H. Zhang, Z.-Z. He and W.-D. Cheng, *Chem. Mater.*, 2013, **26**, 1093.
11 G. Zhang, Y. Li, K. Jiang, H. Zeng, T. Liu, X. Chen, J. Qin, Z. Lin, P. Fu, Y. Wu and C. Chen, *J. Am. Chem. Soc.*, 2012, **134**, 14818.
12 A. S. Haynes, F. O. Saouma, C. O. Otieno, D. J. Clark, D. P. Shoemaker, J. I. Jang and M. G. Kanatzidis, *Chem. Mater.*, 2015, **27**, 1837.
13 D. Mei, W. Yin, L. Bai, Z. Lin, J. Yao, P. Fu and Y. Wu, *Dalton Trans.*, 2011, **40**, 3610.
14 D. Mei, W. Yin, K. Feng, Z. Lin, L. Bai, J. Yao and Y. Wu, *Inorg. Chem.*, 2012, **51**, 1035.
15 H. Lin, L. Chen, L. J. Zhou and L. M. Wu, *J. Am. Chem. Soc.*, 2013, **135**, 12914.
16 Y. Kim, I. S. Seo, S. W. Martin, J. Baek, P. S. Halasyamani, N. Arumugam and H. Steinfink, *Chem. Mater.*, 2008, **20**, 6048.
17 Z. H. Kang, J. Guo, Z. S. Feng, J. Y. Gao, J. J. Xie, L. M. Zhang, V. Atuchin, Y. Andreev, G. Lanskii and A. Shaiduko, *Appl. Phys. B*, 2012, **108**, 545.
18 V. P. Sachanyuk, G. P. Gorgut, V. V. Atuchin, I. D. Olekseyuk and O. V. Parasyuk, *J. Alloys Compd.*, 2008, **452**, 348.
19 I. Chung, J. H. Song, J. I. Jang, A. J. Freeman, J. B. Ketterson and M. G. Kanatzidis, *J. Am. Chem. Soc.*, 2009, **131**, 2647.
20 M.-J. Zhang, X.-M. Jiang, L.-J. Zhou and G.-C. Guo, *J. Mater. Chem. C*, 2013, **1**, 4754.
21 K. Wu, Z. Yang and S. Pan, *Inorg. Chem.*, 2015, **54**, 10108.
22 J. A. Brant, D. J. Clark, Y. S. Kim, J. I. Jang, J.-H. Zhang and J. A. Aitken, *Chem. Mater.*, 2014, **26**, 3045.
23 M. V. Shevchuk, V. V. Atuchin, A. V. Kityk, A. O. Fedorchuk, Y. E. Romanyuk, S. CaŁus, O. M. Yurchenko and O. V. Parasyuk, *J. Cryst. Growth*, 2011, **318**, 708.
24 S. Zhang, D. Mei, X. Du, Z. Lin, J. Zhong, Y. Wu and J. Xu, *J. Solid State Chem.*, 2016, **238**, 21.
25 D. Mei, P. Gong, Z. Lin, K. Feng, J. Yao, F. Huang and Y. Wu, *CrystEngComm*, 2014, **16**, 6836.
26 X. Lin, G. Zhang and N. Ye, *Cryst. Growth Des.*, 2009, **9**, 1186.
27 L. Isaenko, A. Yelisseyev, S. Lobanov, A. Titov, V. Petrov, J. J. Zondy, P. Krinitsin, A. Merkulov, V. Vedenyapin and J. Smirnova, *Cryst. Res. Technol.*, 2003, **38**, 379.
28 J. Yao, D. Mei, L. Bai, Z. Lin, W. Yin, P. Fu and Y. Wu, *Inorg. Chem.*, 2010, **49**, 9212.
29 K. Wu, Z. Yang and S. Pan, *Angew. Chem., Int. Ed.*, 2016, **55**, 6713.
30 L. Kang, M. Zhou, J. Yao, Z. Lin, Y. Wu and C. Chen, *J. Am. Chem. Soc.*, 2015, **137**, 13049.
31 S. K. Kurtz and T. T. Perry, *J. Appl. Phys.*, 1968, **39**, 3798.
32 G. Li, K. Wu, Q. Liu, Z. Yang and S. Pan, *J. Am. Chem. Soc.*, 2016, **138**, 7422.
33 G. M. Sheldrick, *Acta Crystallogr., Sect. A: Found. Crystallogr.*, 2008, **64**, 112.
34 A. L. Spek, *J. Appl. Crystallogr.*, 2003, **36**, 7.
35 P. Hohenberg and W. Kohn, *Phys. Rev.*, 1964, **136**, B864.
36 W. Kohn and L. J. Sham, *Phys. Rev.*, 1965, **140**, A1133.
37 H. J. Monkhorst and J. D. Pack, *Phys. Rev. B: Condens. Matter Mater. Phys.*, 1976, **13**, 5188.
38 W. Carrillo-Cabrera, K. Peters, H. G. von Schnering, F. Menzel and W. Brockner, *Z. Anorg. Allg. Chem.*, 1995, **621**, 557.
39 D. Mei, Z. Lin, L. Bai, J. Yao, P. Fu and Y. Wu, *J. Solid State Chem.*, 2010, **183**, 1640.
40 V. Petrykin, M. Okube, H. Yamane, S. Sasaki and M. Kakihana, *Chem. Mater.*, 2010, **22**, 5800.
41 S. Jörgens, D. Johrendt and A. Mewis, *Z. Anorg. Allg. Chem.*, 2002, **628**, 1765.
42 T. K. Bera, R. G. Iyer, C. D. Malliakas and M. G. Kanatzidis, *Inorg. Chem.*, 2013, **52**, 11370.
43 M.-C. Chen, L.-M. Wu, H. Lin, L.-J. Zhou and L. Chen, *J. Am. Chem. Soc.*, 2012, **134**, 6058.

44 T. K. Bera, J. I. Jang, J. B. Ketterson and M. G. Kanatzidis, *J. Am. Chem. Soc.*, 2009, **131**, 75.
45 D. Mei, W. Yin, Z. Lin, R. He, J. Yao, P. Fu and Y. Wu, *J. Alloys Compd.*, 2011, **509**, 2981.
46 O. Schevciw and W. B. White, *Mater. Res. Bull.*, 1983, **18**, 1059.
47 J. Tauc, R. Grigorovici and A. Vancu, *Phys. Status Solidi*, 1966, **15**, 627.